SCIENCE CHINA
Information Sciences

• RESEARCH PAPERS •
Special Focus

March 2011 Vol. 54 No. 3: 542–550
doi: 10.1007/s11432-011-4196-9

Phugoid dynamic characteristic of hypersonic gliding vehicles

CHEN XiaoQing, HOU ZhongXi, LIU JianXia & CHEN XiaoQian*

College of Aerospace and Materials Engineering, National University of Defense Technology, Changsha 410073, China

Received August 15, 2010; accepted December 16, 2010

Abstract This paper focuses on the phugoid dynamic characteristic of hypersonic gliding vehicle. By regarding equilibrium glide as the fixed state of reentry trajectory, the dynamic equations are simplified and a hyper-geometric equation with a forcing function is deduced. Linearization theory is applied to analyze the characteristic of the motion, and the phugoid mode is found to be stable. An analytical solution of flight path angle as a function of speed is derived based on General Multiple Scale theory. The dynamic characteristic is analyzed, and the analytic solution is found to be in good agreement with the numerical simulation. When the initial states do not satisfy equilibrium glide condition or perturbation occurs, a damped oscillation along the equilibrium glide trajectory would occur. The damping diminishes as the speed decreases. The number of oscillations is decided by the lift-to-drag ratio, the initial altitude and the initial/final speed.

Keywords hypersonic gliding vehicle, phugoid dynamics, equilibrium glide, general multiple scale theory

Citation Chen X Q, Hou Z X, Liu J X, et al. Phugoid dynamic characteristic of hypersonic gliding vehicles. Sci China Inf Sci, 2011, 54: 542–550, doi: 10.1007/s11432-011-4196-9

1 Introduction

Various hypersonic and reentry vehicle technologies are being pursued to enable global reach capability at present [1]. The Force Application Launch from the Continental United States (FALCON) Program [2] and the NASA Next Generation Launch Technology Program Office [3] of the United States government validate both the interest and the need.

Much work has been done to generate/optimize the reentry trajectory [1, 4], while the purpose of this paper is to study the longitudinal dynamics of a lifting vehicle gliding at hypersonic speed such as common aero vehicle (CAV), which is an unmanned aerial vehicle supporting these technologies with the role of "striking from space" [5]. For the purpose of better aerodynamic performance, the basic shape is based on lifting body or waverider configuration.

Because of experiment limitation, the dynamic characteristic of such hypersonic vehicle is investigated using analytical methods. Etkin [6] first analyzed the dynamic stability of hypervelocity aerospace planes. By extending the classical theory of aircraft longitudinal dynamics to the case of hypervelocity orbital flight, he investigated the perturbed motion of a lifting, thrusting vehicle on a circular orbit in the outer fringes of the Earth's atmosphere (30–200 km). Rangi [7] extended Etkin's results by including certain

*Corresponding author (email: gkbatchelor@gmail.com)

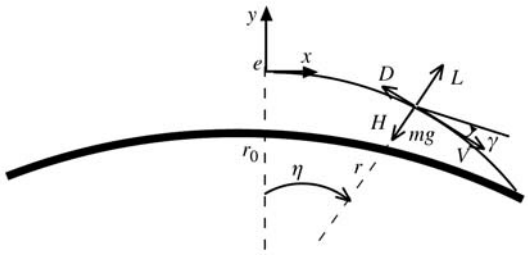

Figure 1 Axis system and nomenclature.

nonlinear terms in the linearized equations and studying their effects on the perturbed vehicle motion. He also found that the effects of the nonlinear terms considered were negligible. Laitone [8] obtained analytical solutions of the linearized equations and compared them with Etkin's numerical results. He found that the phugoid relations were in excellent agreement with the numerical calculations presented by Etkin. Vinh [9, 10] studied the dynamic stability of shuttle vehicle systematically. He analyzed the phugoid oscillations during planar reentry maneuvers of single-stage-to-orbit vehicles and obtained an explicit formula for the number of phugoid oscillations [11].

Berry [12] and Sachs [13, 14] used root-locus method to investigate how jet and rocket engine affect the longitudinal stability of Space Shuttle and NASP (national aerospace plane program). Ferreira [15] studied the nonlinear, unsteady cases of actual atmospheric planetary entry, viz., ballistic and gliding entries. He found that for gliding entry, the two longitudinal modes (phugoid and pitching) are governed by the same general type of equation, viz., forced hypergeometric equation. In ballistic entry, on the contrary, that will not happen.

This paper is dedicated to the phugoid dynamics of high lift-to-drag ratio vehicles gliding at hypersonic speed. The solution of equilibrium glide is analyzed, when the initial state does not satisfy the equilibrium glide condition or perturbation occurs, the dynamic characteristic is analyzed through linearization and generalized multiple scales methods. The analysis show that the vehicle would restore to the equilibrium state as a damping oscillator and the oscillating amplitude fade down as the speed decreases.

2 Dynamic equation analysis

This study focuses on the reentry dynamics of hypersonic gliding vehicle; it is assumed that the vehicle motion takes place around a non-rotating, spherical, homogeneous earth, with a static atmosphere, and the side slip angle is zero. Then the reentry motion would be a planar motion without side force.

2.1 Equations of motion

Based on the assumption above, a coordinate system e-xy which is determined by the vector of initial position r_0 and speed V_0 is established, as shown in Figure 1.

For simplicity, the dynamic equations are listed as eqs. (1a)–(1d). In a planet centric inertial reference frame, the longitudinal dynamic equations [15, 16] are

$$\frac{dr}{dt} = V\sin\gamma, \tag{1a}$$

$$\frac{dV}{dt} = -\frac{D}{m} - g\sin\gamma, \tag{1b}$$

$$\frac{d\gamma}{dt} = \frac{L}{mV} + \frac{1}{V}\left(\frac{V^2}{r} - g\right)\cos\gamma, \tag{1c}$$

$$\frac{d\eta}{dt} = \frac{V}{r}\cos\gamma, \tag{1d}$$

where r measures the radial distance from the earth's center, V is the speed along the trajectory, γ is the flight path angle, η is the range angle, g is the acceleration of gravity, m the vehicle's mass, and D and L are the aerodynamic drag and lift force.

The problem of longitudinal dynamics for reentry is formulated as follows. The initial condition at entry is

$$t = 0, r = r_0,\ V = V_0,\ \gamma = \gamma_0,\ \eta = 0. \tag{2}$$

Let H be the altitude measured from the reference level, and let h be its normalized value, that is,

$$H = r - r_0,\ h = \frac{H}{r_0}. \tag{3}$$

Then

$$\frac{r}{r_0} = 1 - h + h^2 - \cdots \tag{4}$$

For a central Newtonian gravitational attraction, we have

$$\frac{g}{g_0} = \left(\frac{r_0}{r}\right)^2 \simeq 1 - 2\frac{\Delta r}{r_0} = 1 - 2h + 3h^2 - \cdots \tag{5}$$

Since in the relevant terms, the reentry altitude is about 100 km, h is the order of 10^{-2}, during reentry we take $r/r_0 \approx 1$ and $g/g_0 \approx 1$. In addition, to simplify the analytical process, we assume that γ is small, so that $\cos\gamma \simeq 1$ and $\sin\gamma \simeq \gamma$. For example, when $|\gamma| \leqslant 8^\circ$ (in degree) or $|\gamma| < 0.1396$ (in radian), $|\gamma - \sin\gamma| < 0.001$ and $|\cos\gamma - 1| < 0.01$; we use γ and 1 to replace $\sin\gamma$ and $\cos\gamma$.

The atmosphere density ρ is assumed to be a simple exponential, i.e. not broken up into multiple layers. The density is ρ_{sl} at the Earth surface, so

$$\rho = \rho_{sl}\mathrm{e}^{-\beta H}, \tag{6}$$

where β is the density decay constant. So in differential form, we have

$$d\rho = -\beta \cdot \rho \cdot dH. \tag{7}$$

Substituting (7) into (1a), we get

$$\frac{d\rho}{dt} = \beta \cdot \rho \cdot V \cdot \gamma. \tag{8}$$

2.2 The equilibrium glide analysis

The standard glide mode for the long-range, hypersonic vehicle is the equilibrium glide, in which the aerodynamic lift is used to balance the combined gravitational and centrifugal forces.

$$\frac{1}{2}\rho V^2 S C_L = mg\left(1 - \frac{V^2}{gr}\right). \tag{9}$$

This means that the flight path angle is very small and nearly constant during the descent, which means that $\sin\gamma \simeq \gamma$ and $\cos\gamma \simeq 1$. Then the equilibrium solution is (see [15])

$$\rho = \frac{2m(1-u)}{SC_L ru}, \tag{10}$$

$$\gamma = -\frac{2(1-u)}{K(2 + \beta ru(1-u))}, \tag{11}$$

where K is the lift-to-drag ratio and $u = \frac{V^2}{gr}$ is the dimensionless speed in terms of the kinetic energy.

When $u \in [0.01, 0.99]$, the term $\beta ru(1-u) \gg 2$, so the flight path angle, as a function of speed, can be approximated by

$$\gamma = -\frac{2}{K\beta ru}. \tag{12}$$

Figure 2 shows the variation of flight path angle for equilibrium glide as a function of the dimensionless speed. The numerical simulation and the analytical solution are nearly identical down to a very low speed. When the dimensionless speed decreases to 0.05, the flight path angle is -1.69° for $K = 1.5$ and -0.85° for $K = 3$, which means that the small flight path angle assumption is reasonable and the analytic solution can be accepted.

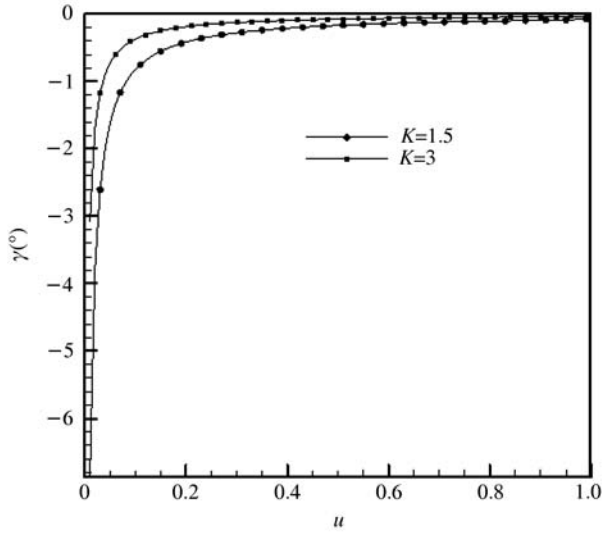

Figure 2 Variation of flight path angle during equilibrium glide.

Remark. The relationship equation (9) could also be obtained by setting $\frac{d\gamma}{dt} = 0$, so from the view point of nonlinear dynamics, the equilibrium glide is the fixed state of hypersonic reentry motion.

3 Stability of phugoid motion in equilibrium glide

Subsection 2.2 provides the analytical solutions for equilibrium glide of hypersonic reentry. For most hypersonic vehicles, the initial states do not satisfy the equilibrium glide conditions. This section discusses the analytical solutions when there is a small initial deviation, either in speed or the flight path angle, or both.

For simplicity, neglecting the small gravity component in eq.(1b), we divide (1a) and (1c) by (1b). The dynamic equations are translated into

$$\frac{d\rho}{dV} = -\frac{2m \cdot \beta \cdot \gamma}{C_D \cdot V \cdot S}, \tag{13a}$$

$$\frac{d\gamma}{dV} = \frac{K}{V} + \frac{2m}{\rho \cdot C_D \cdot S \cdot V^3}\left(\frac{V^2}{r} - g\right)\cos\gamma. \tag{13b}$$

We now introduce dimensionless variables to simplify the equations. In addition to the dimensionless speed u, the density is represented by Chapman's altitude variable (see [15]):

$$Y = \frac{\rho S C_D}{m}\sqrt{\frac{r}{\beta}}, \tag{14}$$

while the flight path angle is analyzed in the form of the dimensionless variable

$$\varphi = -\sqrt{\beta r}\gamma. \tag{15}$$

Then the equilibrium glide flight path angle solution (12) is can be rewritten as

$$\varphi = \frac{2}{\omega u}, \tag{16}$$

where

$$\omega = K\sqrt{\beta r_0}. \tag{17}$$

And eqs. (13a) and (13b) can be rewritten as

$$\frac{dY}{du} = -\frac{\varphi}{u}, \tag{18a}$$

$$\frac{d\varphi}{du} = \frac{\omega}{2u} - \frac{1-u}{u^2 Y}\cos\left(\frac{\varphi}{\sqrt{\beta r_0}}\right). \tag{18b}$$

3.1 Linearization analysis

In this section, we first linearize eqs. (18a) and (18b) in the neighbored of equilibrium points. Let $\xi_1 = Y - Y_s, \xi_2 = \varphi - \varphi_s$ where Y_s and φ_s stand for the equilibrium states. Then the equations could be rewritten as

$$\begin{aligned} \dot{\xi}_1 &= a_{11}\xi_1 + a_{12}\xi_2, \\ \dot{\xi}_2 &= a_{21}\xi_1 + a_{22}\xi_2 \end{aligned} \tag{19}$$

with $a_{11} = 0$, $a_{12} = -\frac{1}{u}$, $a_{21} = \frac{1-u}{u^2Y^2}\cos(\frac{\varphi}{\sqrt{\beta r_0}})$, $a_{22} = \frac{1-u}{u^2Y\sqrt{\beta r_0}}\sin(\frac{\varphi}{\sqrt{\beta r_0}})$.

The trace of the coefficient matrix is

$$T = a_{11} + a_{22} > 0. \tag{20}$$

And the determinant of the coefficient matrix is

$$\Delta = a_{11}a_{22} - a_{12}a_{21} > 0. \tag{21}$$

So

$$\begin{aligned} T^2 - 4\Delta &= \left(\frac{1-u}{u^2Y\sqrt{\beta r_0}}\sin\left(\frac{\varphi}{\sqrt{\beta r_0}}\right)\right)^2 - 4\frac{1-u}{u^3Y^2}\cos\left(\frac{\varphi}{\sqrt{\beta r_0}}\right) \\ &= \frac{1-u}{u^3Y^2}\left(\frac{1-u}{u\sqrt{\beta r_0}}\sin^2\left(\frac{\varphi}{\sqrt{\beta r_0}}\right) - 4\cos\left(\frac{\varphi}{\sqrt{\beta r_0}}\right)\right). \end{aligned} \tag{22}$$

$T^2 - 4\Delta < 0$ while $u \in [0.01, 0.99]$ and $\varphi = \frac{2}{\omega u}$. According to equilibrium point theory, the equilibrium point is an unsteady focus and the amplitude increases exponentially, with an exponent of $T/2$. But in reality, the dimensionless speed decreases from 0.99 to 0.01, so in this sense, the equilibrium point is a steady focus. Any small deviation from the equilibrium glide would result in an oscillation and the amplitude decreases as the speed decreases.

3.2 GMS theory analysis

The general multiple scales (GMS) theory developed by Ramnath [17] is an asymptotic approach for approximating solutions for linear and nonlinear time-varying systems. The GMS theory has been used to study dynamics of various applications [18–20].

3.2.1 *Second-order GMS solution*

Consider the second order LTV differential equation:

$$\frac{d^2y}{dt^2} + Z_1(t)\frac{dy}{dt} + Z_0(t)y = 0. \tag{23}$$

The characteristic roots which describe the solution of eq. (23) are given by the second order algebraic equation:

$$S^2 + Z_1S + Z_0 = 0. \tag{24}$$

As developed by Ramnath, the GMS solution for eq. (23) can be described by two time scales. The fast part of the solution provides frequency information and the slow part provides correction for the amplitude. The GMS solution for eq. (23) is given by

$$y(t) = y_s(t)y_f(t), \tag{25}$$

where the fast solution is

$$y_f(t) = C_1 e^{\int_{t_0}^{t_1} K_r(t)dt}\sin\left(\int_{t_0}^{t_1} K_i(t)dt\right) + C_2 e^{\int_{t_0}^{t_1} K_r(t)dt}\cos\left(\int_{t_0}^{t_1} K_i(t)dt\right) \tag{26}$$

and the slow solution is

$$y_s(t) = |4Z_0(t) - Z_1(t)^2|^{-1/4}, \tag{27}$$

K_i and K_r are the imaginary and real parts of the characteristic roots of eq. (24), respectively. Based on the initial condition, unknown parameters C_1 and C_2 can be determined.

3.2.2 *GMS analysis*

Taking the derivative of eq. (18b), and using eq. (18a) we can obtain

$$\begin{aligned}\frac{d^2\varphi}{du^2} &= -\frac{\omega}{2u^2}+\frac{2uY-u^2\frac{dY}{du}}{u^4Y^2}-\frac{Y+\frac{dY}{du}}{u^2Y^2}\\ &= -\frac{\omega}{2u^2}+\frac{2-u}{u^3Y}-\frac{1-u}{u^3Y^2}\varphi.\end{aligned} \tag{28}$$

From eq. (18b) we can get

$$\frac{1}{Y}=\frac{u^2}{1-u}\left(\frac{\omega}{2u}-\frac{d\varphi}{du}\right). \tag{29}$$

Substitute expression (29) into eq. (28). Then a second order nonlinear differential equation for φ is obtained:

$$u(1-u)\frac{d^2\varphi}{du^2}-u\frac{d\varphi}{du}+\frac{\omega^2}{4}\varphi=\frac{\omega}{2u}-(2-\omega\varphi u)\frac{d\varphi}{du}-\varphi u^2\left(\frac{d\varphi}{du}\right)^2. \tag{30}$$

An equilibrium glide path would be observed if the initial conditions satisfy expressions (10) and (11). Here we analyze the dynamic characteristics when there are small initial deviations from equilibrium glide state, either in the speed or in the flight path angle, or both. Using the reference solution (12) to evaluate the last two terms $-(2-\omega\varphi u)\frac{d\varphi}{du}-\varphi u^2(\frac{d\varphi}{du})^2$, we obtain $-8/\omega^3u^2$, which can be neglected compared to $\omega/2u$. Therefore, in liberalized form, eq. (30) becomes

$$u(1-u)\frac{d^2\varphi}{du^2}-u\frac{d\varphi}{du}+\frac{\omega^2}{4}\varphi=\frac{\omega}{2u}. \tag{31}$$

Therefore, the flight path angle is governed by a hyper-geometric equation with a forcing term in gliding entry. Here we will apply GMS theory to analyze the characteristic of the motion.

First, normalize eq. (31) as

$$\frac{d^2\varphi}{du^2}-\frac{1}{1-u}\frac{d\varphi}{du}+\frac{\omega^2}{4u(1-u)}\varphi=\frac{\omega}{2u^2(1-u)}. \tag{32}$$

The characteristic roots of eq. (32) are

$$\begin{aligned}K_r(u)&=\frac{1}{2(1-u)},\\ K_i(u)&=\frac{1}{2}\sqrt{\frac{\omega^2(1-u)-u}{u(1-u)^2}}\approx\frac{\omega}{2\sqrt{u(1-u)}}.\end{aligned} \tag{33}$$

So the fast solution is

$$\varphi_f(u)=C_1\mathrm{e}^{\int_{u0}^{u}K_r(u)du}\sin\left(\int_{u0}^{u}K_i(u)du\right)+C_2\mathrm{e}^{\int_{u0}^{u}K_r(u)du}\cos\left(\int_{u0}^{u}K_i(u)du\right)$$

and the slow solution is

$$\varphi_s(u)=(u(1-u)/\omega^2)^{1/4}. \tag{34}$$

The GMS solution is

$$\varphi=\varphi_s\varphi_f=\left(\frac{u(1-u)}{\omega^2}\right)^{\frac{1}{4}}\mathrm{e}^{-\frac{1}{2}\ln\frac{1-u}{1-u_0}}f(u), \tag{35}$$

where

$$f(u)=C_1\sin\left(\frac{\omega}{2}(\arccos(1-2u)-\arccos(1-2u_0))\right)+C_2\cos\left(\frac{\omega}{2}(\arccos(1-2u)-\arccos(1-2u_0))\right), \tag{36}$$

$f(u)$ is a periodic function. Considering the neglected item $\frac{\omega}{2u^2(1-u)}$, the complete solution (= equilibrium + perturbation) for the flight path angle is

$$\varphi=\frac{\omega/2u^2(1-u)}{\omega^2/4u(1-u)}+\left(\frac{u(1-u)}{\omega^2}\right)^{\frac{1}{4}}\mathrm{e}^{-\frac{1}{2}\ln\frac{1-u}{1-u_0}}f(u)$$

$$= \frac{2}{\omega u} + \sqrt{\frac{1-u_0}{\omega}}\left(\frac{u}{1-u}\right)^{\frac{1}{4}} f(u). \tag{37}$$

It is clear the first item is equilibrium glide solution. When the vehicle glides along the reference equilibrium glide trajectory, $C_1 = C_2 = 0$ and the flight path angle decreases continuously as the speed decreases. When a perturbation occurs, φ undergoes an oscillation and the damping is provided by the following function:

$$\xi(u) = u^{1/4}(1-u)^{-1/4}. \tag{38}$$

Expression (38) is the same as that Ferreira developed in [15] while he derived it through Liouville's transformation. The dimensionless density Ycan be obtained as

$$\begin{aligned}\frac{1}{Y} &= \frac{u^2}{1-u}\left(\frac{\omega}{2u} - \frac{d\varphi}{du}\right)\\ &= \frac{u^2}{1-u}\left[\begin{array}{l}\dfrac{\omega}{2u} + \dfrac{2}{\omega u^2}\\ -\sqrt{\dfrac{1-u_0}{\omega}}\left(\begin{array}{l}\dfrac{\omega(\frac{u}{1-u})^{1/4}}{\sqrt{1-(1-2u)^2}}\left(C_1\cos\left(\dfrac{\omega}{2}\arccos(1-2u)\right)\right.\\ \left.+C_2\sin\left(\dfrac{\omega}{2}\arccos(1-2u)\right)\right)\\ +\dfrac{1}{4(1-u)^{5/4}u^{3/4}}\left(C_1\sin\left(\dfrac{\omega}{2}\arccos(1-2u)\right)\right.\\ \left.+C_2\cos\left(\dfrac{\omega}{2}\arccos(1-2u)\right)\right)\end{array}\right)\end{array}\right].\end{aligned} \tag{39}$$

The first item gives the equilibrium glide solution; the second item is very small compared to the first item while the last item provides the damped oscillatory perturbation.

3.3 Damping characteristic

From the analysis above, it is known that when the initial states do not satisfy the equilibrium glide condition, the flight path angle would oscillate along the equilibrium glide trajectory and the amplitude decreases as the speed decreases. When the deviation from the equilibrium glide state is too large, the speed would not decrease monotonously at the early stage, and the analytical expression could forecast the damping oscillation but it is hard to give an accurate solution.

Figure 3 presents the plot of height and flight path angle as a function of dimensionless speed with different initial states: u_0=0.95, γ_0=0, H_0=80 km and u_0=0.9, γ_0=0, H_0=80 km with $K = 3$. The equilibrium states at H_0=80 km are u=0.9865 and $\gamma = -0.0367°$. Compared with equilibrium glide trajectory, when perturbation occurs and the states do not satisfy the equilibrium glide condition, the trajectory would be a skip trajectory along the equilibrium glide trajectory, and the larger the perturbation, the larger the amplitude.

The damping characteristic of the dimensionless variable φ is depicted by eq. (37), which depends on the dimensionless speed only. When considering the flight path angle γ, the factor $\sqrt{\beta r}$ used in eq. (15) should be considered. Figure 4 shows the plot of damping characteristic, which appears that the eq. (37) correctly predicts the damping in the equilibrium glide mode. It should be noted that the damping characteristic is rescaled by the maximum oscillation amplitude.

3.4 Oscillation number analysis

As analyzed above, when perturbation occurs, or the initial states do not satisfy equilibrium glide condition (eqs. (10) and (11)), the trajectory would oscillate along the equilibrium glide trajectory. This part would analyze the number of oscillations, viz. the characteristic of function (36), and furthermore, function $\arccos(1-2u)$.

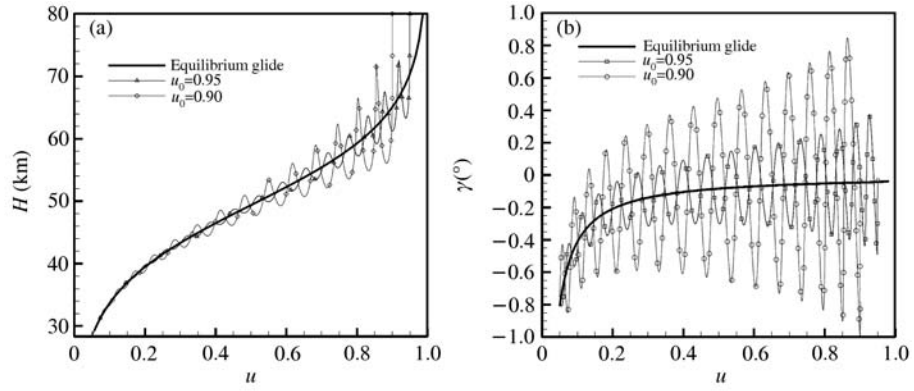

Figure 3 Variation of altitude and flight path angle during gliding reentry. (a) Altitude-dimensionless speed; (b) flight path angle-dimensionless speed.

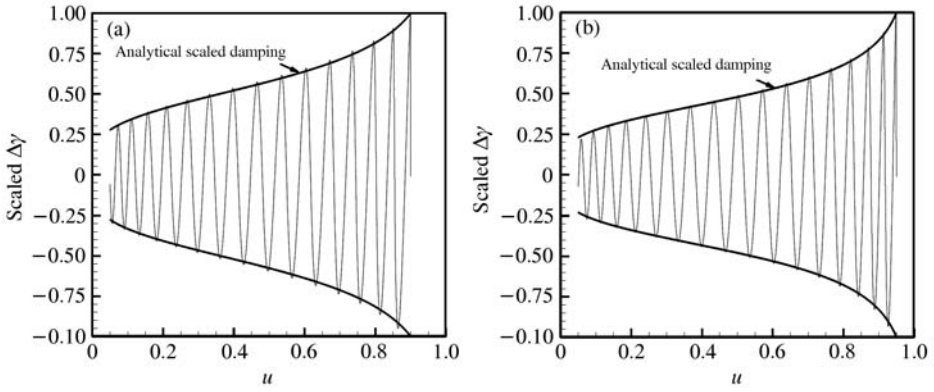

Figure 4 Damping characteristic. (a) $u_0 = 0.9$, $\gamma_0 = 0$, H_0=80 km; (b) $u_0 = 0.95$, $\gamma_0 = 0$, H_0=80 km.

As has been mentioned previously, u varies from 1 to 0, which means that $\arccos(1-2u)$ varies from $-\pi/2$ to $\pi/2$. Thus, over the complete range of the speed the number of oscillations with frequency w is computed by

$$N = \frac{\frac{\omega}{2} \times \pi}{2\pi} = \frac{\omega}{4} = \frac{\sqrt{\beta r_0}}{4} K. \tag{40}$$

The number of oscillations is proportional to the lift to drag ratio K. As a numerical example, N=11.3 while K=1.5 and N = 22.6 while K=3. The initial altitude also affects the number of oscillations, but numerical calculation shows that the influence can be neglected.

Given the initial and final dimensionless speed u_i and u_e, the number of oscillations is

$$N = \frac{K\sqrt{\beta r_0}}{4\pi} \times |\arccos(1-2u_e) - \arccos(1-2u_i)|. \tag{41}$$

Using fourth order Runge-Kutta methods to solve the ordinary differential eqs. (1a)–(1d) numerically, we count the number of oscillation. Table 1 gives the calculation results with different u_i but the same $u_{\rm e} = 0.05$ with the initial states H_0=80 km, $\gamma_0 = 0°$. The numerical result is calculated by rounding method which causes the difference. From Table 1, it can be concluded that the analytical expression (41) can be accepted with a high reliability.

As to the period of oscillation, because the fly time is different with different initial states and the function $\cos(\frac{\omega}{2}\arccos(1-2u))$ is nonlinear, the frequency and the period of $f(u)$ is not a constant. We use average period to estimate the period of phugoid:

$$T = \frac{t}{N}, \tag{42}$$

where t is the fly time and N is the number of oscillation. In the case K = 3, h_0=80 km, u_i = 0.95, $\gamma_0 = 0°$ and $u_{\rm e} = 0.05$, the fly time is 5000 s, the average period is about 300 s.

Table 1 Oscillation number

u_0	Numeric	Analytic
0.97	17	16.7
0.95	17	16.1
0.93	16	15.4
0.92	16	15.2
0.90	15	14.6

4 Conclusions

The phugoid dynamics of hypersonic glide vehicle is analyzed theoretically using general multiple scale theory and the following conclusions can be obtained:

Equilibrium glide is the fixed state of hypersonic glide vehicle, when the initial states do not satisfy equilibrium glide condition or perturbation occurs, a damped oscillation along the equilibrium glide trajectory, viz. skip trajectory, could be observed.

Dimensionless speed is one of the parameters that influence the damping characteristic, and the damping diminishes as the speed decreases, and the analytical solution agrees well with the numerical simulation.

The number of oscillations is decided by the lift-to-drag ratio, the initial altitude and the initial/final speed. The initial altitude's influence can be neglected and the number of oscillations is proportional to the lift-to-drag ratio.

Acknowledgements

This work was supported by the National Natural Science Foundation of China (Grant Nos. 90916016, 50975280), and Hunan Provincial Innovation Foundation for Postgraduate.

References

1 Timothy R J, Cobb R G. Three-dimensional trajectory optimization satisfying waypoint and no-fly zone constraints. J Guid Control Dyn, 2009. 32: 551–572
2 DARPA. FALCON force application and launch from CONUS. BAA 03–35. 2004
3 Hueter U, Hutt J J. NASA's next generation launch technology program-next generation space access roadmap. AIAA 2003–6941. 2003
4 Bollino K P. High-fidelity real-time trajectory optimization for reusable launch vehicles. Dissertation for the Doctoral Degree. California: Naval Postgraduate School. 2006
5 Richie G. The common aero vehicle: space delivery system of the future. AIAA 99-4435. 1999
6 Etkin B. Longitudinal dynamics of a lifting vehicle in orbital flight. J Aerosp Sci, 1961, 28: 779–788
7 Rangi R S. Non-linear effects in the longitudinal dynamics of a lifting vehicle in orbital flight. UTIA TN-40, 1960
8 Laitone E V, Chou Y S. Phugoid oscillations at hypersonic speeds. AIAA J, 1965, 3: 732–737
9 Vinh N X. Longitudinal dynamics stability of a shuttle vehicle. AIAA 70-977. 1970
10 Vinh N X. Hypersonic and planetary entry flight mechanics. Ann Arbor: the University of Michigan Press, 1980
11 Vinh N X, Chern J S, Lin C F. Phugoid oscillations in optimal reentry trajectorie. Acta Astronaut, 1981, 8: 311–324
12 Berry D T. National aerospace plane longitudinal long-period dynamics. J Guid Control Dyn, 1991, 14: 205–206
13 Sachs G. Effect of thrust/speed dependence on long-period dynamics in supersonic flight. J Guid Control Dyn, 1990, 13: 1163–1166
14 Sachs G. Thrust/speed effects on long-term dynamics of aerospace planes. J Guid Control Dyn, 1992, 15: 1050–1053
15 Ferreira L de O. Nonlinear dynamics and stability of hypersonic reentry vehicles. Dissertation for the Doctoral Degree. Michigan: University of Michigan, 1995
16 Snell S A. Nonlinear dynamic-inversion flight control of supermaneuverable aircraft. Twin Cities: University of Minnesota, 1991
17 Ramnath R V, Sandri G. A Generalized multiple scales approach to a class of linear differential equation. J Math Anal Appl, 1969, 28: 229–364
18 Ramnath R V, Sinha P. Dynamics of the space shuttle during entry into earth's atmosphere. AIAA J, 1975, 13:
19 Tao Y. Satellite attitude prediction by multiple time scales method. Massachusetts Institute of Technology. Dissertation for the Doctoral Degree. 1976
20 Radovsky S E. Sensitivity analysis of slowly-varying systems as applied to a VTOL airplane. Dissertation for the Master Degree. Cambridge: Massachusetts Institute of Technology, 1978